OBSERVATION, ANALYSIS AND MODELING OF THE SEA BREEZE CIRCULATION DURING THE NOAA/ARL-JSU METEOROLOGICAL FIELD EXPERIMENT SUMMER 2009

William R. Pendergrass, LaToya Myles, Christoph A. Vogel
(NOAA/Air Resources Laboratory/Atmospheric Turbulence & Diffusion Division, Oak Ridge, TN)
and
Venkata Bhaskar Rao Dodla, Hari Prasad Dasari, Anjaneyulu Yerramilli*, Julius M Baham, Robert Hughes, Chuck Patrick, John Young, and Shelton Swanier
(Trent Lott Geospatial Visualization Research Centre, Jackson State University, Jackson MS 39204, USA)

ABSTRACT

In this study an attempt is made to simulate the diurnal variations of the coastal land and sea breeze atmospheric circulations over the Mississippi Gulf Coast region. It is known that the characteristics of the coastal circulations are dependent on the local topography and land use patterns and the Mississippi Gulf Coast region assumes importance due to its complex terrain features and land use and houses number of industries.

Observations collected at the locations of Harrison County School and Wiggins Airport, situated normal to the Mississippi Gulf Coast region, during June-2009 as a joint NOAA-ARL and JSU-TLGVRC field experiment, were analyzed to understand the characteristics of the sea breeze circulation. These comprise radio-sonde observations collected at 5 times of 0900, 1100, 1300, 1500 and 1700 CST (local US time) for four consecutive days of 16 to 19 June, 2009. The main objective of this field experiment was to study the coastal boundary layer structure associated with the development of sea breeze circulation. During this period, radio-sonde observations were collected at the two locations, normal to the Mississippi Gulf Coast, of Harrison County School (30.5N,89.1W) and Wiggins Airport (30.8N,89.13W) at five times (i.e.) 1400, 1600, 1800, 2000 and 2200 UTC daily.

For the modeling part, a high resolution mesoscale model, ARW (Advanced Research WRF), was used to simulate the boundary layer characteristics associated with the sea breeze circulation over the Gulf Coast Region corresponding to this 4-day period. The model was designed to have nested two-way interactive three domains with 36, 12 and 4 km resolutions, with the inner most domain covering the entire Gulf Coast region, and 41 vertical levels of which 30 levels were chosen to be below 500 hPa level so as to fine resolve the boundary layer features. The initial and boundary conditions were provided from NCEP FNL data available at 1 degree interval and the boundary conditions were updated at every 6 hours. The model was integrated for 48 hours starting from 00 and 12 UTC of each day starting from 15 June up to 00 UTC of 18 June 2009.

The model simulated atmospheric fields were used to derive the wind, temperature and humidity parameters corresponding to the two locations and the available observation times. The model results were compared with corresponding observations for validation. The model could simulate the gradual development and strengthening of the sea breeze with the progress of daytime. The model could also simulate the variations in the sea breeze at the two locations which are separated by about 25 miles. From the model output, the horizontal and vertical extent of the sea breeze circulation at different time during the daytime period could be identified. The temperature and humidity variations associated with the sea breeze circulation over the Gulf Coast region were also analyzed. These features were compared with the observations collected at the two locations of Harrison County School and Wiggins Airport. These features are noted to have good correspondence with the observations. This study demonstrates the use of WRF ARW high resolution model in the mesoscale atmospheric prediction applications.

1. INTRODUCTION

The diurnal cycle of winds over the coastal regions is a characteristic feature with onshore winds during daytime and offshore winds during night. This wind regime is generally referred to as the sea and land breeze circulation. It is generally observed that daytime sea breeze is stronger than night time land breeze. Such differences in wind speed are due to the amplitude of the land-sea temperature gradients. These differences are apparent when synoptic scale winds are weak. The reasons for non-uniform change of sea breeze direction with time is attributed to the Corilois effect, pressure gradients due to diurnal heating and pressure gradients not affected by diurnal changes (Neumann, 1977). A number of theoretical and numerical modeling studies were attempted to simulate and understand the characteristics of the land and sea breeze circulations (Estoque, 1961; Mak and Walsh, 1976; Zhong and Takle, 1993; Simpson, 1996). Due to its importance, observational and modeling studies of sea breeze characteristics over different regions were attempted (Abbs and Physick, 1992; Tijm et al,

*Corresponding author e-mail: yerramilli.anjaneyulu@jsums.edu

1999; Fukuda et al, 2001; Colby, 2004; Drobinski et al, 2006 and Hisada et al, 2009).

Mississippi Gulf Coast region has been chosen for carrying out a special observation program of the meteorological parameters and air quality during the summer of 2009 with a view to understand the characteristics of the sea breeze and the planetary boundary layer as they are important in the computation of pollutants dispersion. NOAA/ARL (National Oceanographic and Atmospheric Administration/ Atmospheric Research Laboratory) and JSU/TLGVRC (Jackson State University/ Trent Lott Geospatial and Visualization Research Center) conducted this joint field experiment during 16-19 June 2009 over the Gulf Port region under which intense observations were collected at two observation sites. The details of this field experiment are given in Section 2. This program was important for the NOAA/ARL funded atmospheric dispersion program at TLGVRC/JSU since 2006 under which extensive modeling efforts are being made to derive the atmospheric dispersion characteristics over the Mississippi Gulf Coast region and to assess the vulnerability of the region to the existing industries.

In this paper the observations that were taken at locations along 89 W, perpendicular to the Gulf Coast, and results from numerical modeling experiments were analyzed to study the sea breeze evolution and to validate the model simulations. For this purpose a high resolution mesoscale atmospheric model was used with a fine horizontal resolution of 4 km and the details of the model and the numerical experiments performed were described in Section 3. The results were described in Section 4 and brief statement of conclusions was given in Section 5.

2. DESCRIPTION OF THE FIELD EXPERIMENT

A joint special observation field experiment was conducted by NOAA/ARL and JSU/TLGVRC for a 5-day period during 16-20 June 2009 near Gulf Port of the Mississippi State. This observation program is taken as a part of the ongoing NOAA sponsored ADP program at JSU/TLGVRC since 2006 and that Mississippi Gulf Coast houses many industries that release pollutants. The ADP program has the main objective of studying the atmospheric dispersion of the important pollutants that are being released and spread in this region affecting the habitants. Radiosonde balloons were released at 5 times during daytime hours of 09, 11, 13, 15 and 17 hours of Central US time, which correspond to 14, 16, 18, 20 and 22 UTC, on all the five days during 16-20 June 2009 at two selected locations. These two locations are Harrison County School (30.5N, 89.1W) and Wiggins Airport (30.8N, 89.13W), which are 30 miles apart on the longitude of 89W and nearly perpendicular to the Gulf Coast (Figure 1a). These observations were planned to probe and study the evolution of sea breeze and the planetary boundary layer characteristics over the Mississippi Gulf Coast region. The Radio-sonde balloons were given ascent so as to reach 12-16 km in about an hour. The sensors attached to the balloon were sending the atmospheric data of temperature and humidity and balloon location through GPS (to yield wind direction and speed) at every 10 sec interval, which is at a vertical resolution of about few tens of meters. The 3-dimensional paths of balloon trajectories from the two locations are shown in Figure 1 (b and c). This raw data was directly loaded into a computer storage system and the vertical profiles of temperature and humidity were continuously updated every 30 sec through use of special meteorology application software (like RAOB). The observations were then subject to a quality control check at NOAA and were made available for analysis.

3. DESCRIPTION OF MODEL AND NUMERICAL EXPERIMENTS

The details of the mesoscale atmospheric model, and the details of the numerical experiments performed are presented in this section.

3a. *Description of Atmospheric Model*

ARW model is used to produce the atmospheric fields at a high resolution over the study region for the desired time period. WRF (Weather Research and Forecasting) mesoscale atmospheric modeling system has been developed and sourced from National Center for Atmospheric Research (NCAR), as the next generation model after MM5, incorporating the advances in atmospheric simulation system suitable for a broad range of applications. WRF is available with two different dynamic cores one as the Advanced Research WRF (ARW) and the other as the Non-hydrostatic Mesoscale Model (NMM). This model system has versatility to choose the domain region of interest; horizontal resolution; interactive nested domains and with various options to choose parameterization schemes for convection, planetary boundary layer (PBL), explicit moisture; radiation and soil processes. ARW is designed to be a flexible, state-of-the-art atmospheric simulation system that is portable and efficient on available parallel computing platforms and a detailed description was provided by Skamarock et al. (2008). ARW is suitable for use in a broad range of applications across scales ranging from meters to thousands of kilometers. ARW model system was used in this study for its accurate numerics, higher order mass conservation characteristics and advanced physics. The model consists of fully compressible non-hydrostatic equations and the prognostic variables include the three-dimensional wind, perturbation quantities of pressure, potential temperature, geo-potential, surface pressure, turbulent kinetic energy and scalars (water vapour mixing ratio, cloud water etc). The model equations are formulated using mass-based terrain following coordinate system, and solved in Arakawa-C grid using Runge–Kutta third order time integration techniques. The model has several options for spatial discretization, diffusion, nesting and lateral boundary conditions. The ARW Solver is the key component of the modeling system, which is composed of several initialization programs for idealized, and real-data simulations, and the numerical integration program. ARW supports horizontal nesting that allows resolution to be focused over a region of interest by introducing an additional grid (or grids) into the simulation with the choice of one-way and two-way nesting procedures. The model system provides a choice of parameterization schemes for physical processes of microphysics, cumulus parameterization, planetary boundary layer (PBL), land surface model and radiation.

3b. *Numerical Experiments*

For the present study, ARW model was configured with three, two-way interactive nested domains, with outer domain at 36 km resolution, middle domain at 12 km resolution and inner domain at 4 km resolution and 42 vertical levels. The details of the design and adaptation of ARW model, for the present study, are given in Table 1 and the model domains are shown in Figure 2. ARW model was integrated for a 48-hour period starting from 00 UTC of each day of 15 to 19 June 2009. The initial and time varying boundary conditions required for the model integrations were taken from NCEP FNL data available at 1 degree interval and at 6-hour interval. The boundary conditions are updated at every 6 hour interval (i.e.) at 00, 06, 12 and 18 UTC during the period of model integration. The model topography and land use for the three model domains were taken from USGS data sources. Model derived outputs were retrieved at 1-hour interval for analyses and validation.

4. Results

In section 3b, it was mentioned that numerical model integrations were performed continuously for a 48-hour period starting from 00 UTC of each day of 15 to 19 June 2009. Though all the model outputs are analyzed, the results of only one day, which is for 18 June 2009, are only presented here. This is to avoid repetition of similar kind of description of the land- sea breeze characteristics prevailing during the special observation program. The authors also state that a large- scale high pressure system was prevailed over the southeast US, including Mississippi Gulf Coast region where the observations were recorded. The observations and the model simulations are described with this back ground large scale circulation feature. A description of the model derived wind flow, temperature and humidity fields over the inner most domain covering the Gulf Coast region at 3 different times (10, 16 and 22 UTC) of 18 June 2009 was presented as the chosen times correspond to 05, 11 and 17 hours of local US time (CDT) which is five hours behind the UTC. Most of the features show contrasting effects of the land and sea regions as the model domain has land region to the north and sea region to the south over the eastern parts of the domain and mostly land part with 10% sea region to south over the western half of the domain.

The surface wind flow (10m) at four different times of 18 June 2009 is presented in Figure 3. At 1000 UTC, clockwise (anticyclonic) wind flow circulation was present over the model domain, with northerlies (easterlies) over the eastern (western) parts of the land region, and northeasterly (easterly) wind flow over eastern (western) parts of the ocean region. The southern parts of the domain, covered by sea, has higher magnitude of winds with values in the range of 10-15 m/s where as the land part has wind flow with strength of 5-10 m/s. At this time of the day, that is 0400 local time, the land breeze is expected to be stronger as land will be cooler (shown in Figure 5). At 1600 UTC, (1100 US CDT), the wind flow regime is nearly same as at 1000 UTC with northerly (northeasterly) flow over land (sea) region on the eastern parts and near easterlies over the western region. However the magnitude of the wind flow is weaker over land with magnitudes of 2-5 m/s appearing over the eastern parts while the strength of wind flow remains as 10-15 m/s over the adjacent sea region towards south. This indicates weakening of the pressure gradient with the land getting heated slowly with day time heating. At 2200 UTC (1700 US CDT), the wind flow is anticlockwise indicating the influence of the prevailing high pressure system. The model simulates increasing wind speed over central parts of the land region with wind strength increasing to 5-10 m/s from 2-5 m/s at 1500 UTC. The wind flow strength decreased to 5-10 m/s over eastern parts of the sea region, which is southeast parts of the model domain, indicating the presence of sea breeze at this time. The decrease of strength in the wind flow from land towards sea (northerly flow) is an indicator of the reversing pressure gradients due to heating of land for nearly 10 hours of daytime. The reversal of wind could not be seen clearly as the large scale anticyclonic flow associated with the high pressure system dominates the local features. The latitude-height vertical section of wind flow along 89 W at 1000, 1600 and 2200 UTC are shown in Figure 4. This figure shows the gradual reduction in strength of easterlies/ north-easterlies over the land region (north of 30N) with increasing daytime. This reduction is due to the influence of sea breeze during daytime. Along this longitude of 89W, the wind speed increases to higher than 15 m/s at 2200 UTC, south of 29 N further indicate the orientation of pressure gradients as from east to west at about 1 km height.

The temperatures and relative humidity (RH) distribution at 985 hPa level (0.2 km) are analyzed and presented in Figure 5. At 1000 UTC, the temperature gradients indicate southwest- northeast orientation, with colder temperatures over land and towards east. Most of the central and eastern parts of the land region has temperatures less than 21 C while the central and western parts of the ocean has temperatures higher than 24 C with high values of 25-26 C over central parts. The influence of ocean is seen over the western parts while the land influence is pronounced over the eastern parts of the sea. Consistent with this, the RH distribution shows moist region over southwest parts and drier region over northeast. The protrusion of higher temperatures with higher RH from sea to land over the south-central parts indicates the effect of warmer sea at this part of the coastline. At 1600 UTC, similar features as of 1000 UTC prevail but with weaker temperature gradients oriented west- east with increase of temperatures all over. The temperatures over western parts of the land reached 24-26 C compared to 22-23 C on eastern parts. This type of change is due to the prevailing high pressure system. The RH values are higher to the south while the values over land decrease due to dry northerly flow from interior land regions due to the prevailing strong northerly flow over eastern parts. At 2200 UTC (1700 CDT), the temperature distribution shows a complete reversal with land part having higher temperatures with values over 27 C, while the sea region temperatures remain around 24-26 C. The western parts of the land region shows the highest temperatures with values exceeding 28 C as compared to 27 C over the central and eastern parts, and with low values of RH with less than 20 %, indicate the effect of subsidence over this region due to the prevailing high pressure system. These features show the dominance of the large scale circulation with high pressure system over the local-scale coastal circulation. The latitude- height vertical section of temperature along 89 W at different times of 1000, 1600 and 2200 UTC of 18 June 2009 are presented in Figure 6. These features show that the variations associated with land- sea breezes are mostly confined to below 900 hPa level. The temperature gradients are oriented from south to north at 1000 UTC, reduced and near neutral at 1600 UTC, reverse as north to south at 2200 UTC. The reversal of the temperature gradients shows the influence of the diurnal variations in land and sea heating characteristic of coastal circulation. The moisture variations show increase of moisture over land, to the north of 30N, with increasing daytime. Low moisture near surface and higher moisture above at 2200 UTC indicate the influence of northerly winds at the surface. The dominance of dry northerly winds slowly reduce with increasing daytime indicate the effect of evolution of sea breeze.

As the second part of this paper, model derived vertical profiles of temperature, relative humidity and wind speed were compared with the observations taken at the two locations of Harrison County School and Wiggins Airport over the Gulf Port. As mentioned in Section 2, observations of temperature, humidity, wind direction and speed were observed through radiosonde balloon ascents at 0900, 1100, 1300, 1500 and 1700 US CDT on all the days during 16-20 June 2009. The model derived fields were taken at the nearest point to the observation location for comparison with observations. Since the model resolution is 4 km, the choice of the nearest grid point is assumed to be reasonable. It is important to note here that the observations are collected at small time intervals during the ascent and so the fields were observed at a very high vertical resolution, often at few tens of meters interval. The model derived fields have a serious limitation of coarse vertical resolution and so may not produce all the observed features.

At Harrison County School (30.5N, 89.1W), the vertical variations of temperature below 600 hPa level at 1400, 1600, 1800 and 2000 UTC are presented in Figure 7. It is noted that the temperature a small inversion layer very near the ground and the height of the inversion gradually increases with progress of daytime. Correspondingly, the model predicts an inversion very near the ground, with inversion agreeing with observations at 1400 UTC. However the increase of inversion height with time could not be predicted by the model. A weak inversion is also noted in the observations at 700 hPa level, and the model could not simulate this weak inversion. However, the model could simulate the inversion very near the ground, and importantly the lapse rate. This figure also shows the differences in the temperature at ground level, as the model underestimates the magnitude during afternoon hours. The vertical profile of RH (Figure 8) shows a good agreement between the model simulation and observations. Though observations show strong variations at certain levels, the general decrease of humidity with height below 700 hPa and increase above was could be simulated by the model. Observations show a sudden increase to 80%, in the afternoon hours, at around 900 hPa level and the same was not simulated by the model. The model also simulates higher RH values at the ground level as compared to observations. Observations of vertical variation of wind speed show sharp changes, such as sudden increase at 900 hPa level and 700 hPa level in the afternoon hours. At these corresponding times, the model simulates an increase around 900 hPa and 700 hPa levels but with lesser magnitude at 900 hPa level and nearly same at 700 hPa level. The model also simulates a decrease in wind speed at 800 hPa level with higher magnitude than observations (Figure 9). The model underestimates the wind speed at lower levels during the forenoon hours. This shows the limitation of the model simulation due to coarse vertical resolution.

At the location of Wiggins Airport, similar features as of Harrison County School are noted. The temperature observations show a low level inversion around 900 hPa (higher level than Harrison County School location) and another weak inversion around 700 hPa level (Figure 10). The model simulates only one inversion at around 950 hPa level. However the lapse rate values have good agreement. For this location also, the near ground temperatures are underestimated during afternoon hours. That indicates the need for improvement in surface layer physics. The model simulated RH profile is in better conformity with observations at 1400, 1600 and 1800 UTC, with the simulation of decrease of RH below 700 hPa and increase above (Figure 11). However at 2000 UTC, observations show a sharp increase of humidity at 900 hPa level, which the model could not simulate at all. As of the vertical variation of wind speed, the model underestimated the magnitude at lower levels at the beginning of the day (i.e.) at 1400 UTC, where as the simulation has better agreement at the other three times at 1600, 1800 and 2000 UTC (Figure 12). At 1400 and 1600 UTC times, the model underestimated the wind speed at levels below 800 hPa level, However, the model could simulate the variations matching with observations during afternoon times. The mode simulates a sharp decrease near 800 hPa level as compared to a decrease near 700 hPa level in the observations.

The above description of the results shows the advantages and the limitations of the model simulation of the land- sea breeze characteristics over the Mississippi Gulf Coast region. Basing on these results, the following conclusions could be made.

5. CONCLUSIONS

1. The model could simulate the onset and evolution of the sea breeze over the Gulf Port region during mid-summer daytime. The model clearly produced the large-scale anti-cyclonic circulation associated with a prevailing high pressure system.
2. The model simulated northerly/ northeasterly wind flow over eastern parts and easterly flow over western parts. The reduction of strength of northerly flow over land region, indicate the effect of sea breeze with the advancement of daytime.
3. The temperature and humidity distributions show heating of the land region, and more warming of the western parts as compared to the east.
4. The model could predict the incursion of moist air above 900 hPa level, indirectly substantiating the ground level inversion that was noted in the observations. This was shown clearly from the vertical section analysis.
5. The effect of sea breeze was shown to be extending up to 800 hPa level in the afternoon.
6. The model has limitations in the prediction of near ground temperatures and humidity values, especially during the afternoon hours. This indicates that the parameterization of the surface layer and boundary layer needs improvement.

7. ACKNOWLEDGMENT

This study is carried out as part of the ongoing Atmospheric Dispersion project (ADP) funded by National Oceanic and Atmospheric Administration (NOAA) through the U.S. Department of Commerce Grant #NA06OAR4600192.

8. REFERENCES

Abbs, D.J. and W.L. Physick, Sea-breeze observations and modeling: a review. *Aust. Met. Mag.* **1992***,41, 7-19.*

Colby Jr, F. P.,. Simulation of the New England sea breeze: The effect of grid spacing. *Wea. Forecast*. **2004**, 19, 277 – 285.

Drobinski,P., S. Bastin, A. Dabas, P. Delville, and O. Reitebuch. Variability of three-dimensional sea breeze structure in southern France: observations and evaluation of empirical scaling l. *Ann. Geophys*. **2006**, 24, 1783–1799.

Estoque, M. A., A theoretical investigation on land and sea breezes. *Quart. J. Roy. Soc. Meteor*. **1961**, 87,. 136-142.

Fukuda, K., N. Matsunaga, and S. Sakai, Behavior of Sea Breeze in Fukuoka. *Annual Journal of Hydraulic Engineering* **2001**, 44, 85-90.

Hisada, Yukiko, Takayoshi Uechi, Nobuhiro Matsunaga, A relationship between the characteristics of sea breeze and land-use in fukuoka metropolitan area. *The seventh International Conference on Urban Climate*, 29 June - 3 July **2009**, Yokohama, Japan.

Mak, K-M, and J.E. Walsh, On the relative intensities of sea and land breezes. *J. Atmos. Sci.* **1976**, 33, 242-251.

Neumann, J., On the rotation of the direction of sea and land breezes. *J. Atmos. Sci* **1977**, 34, 1913-1917.

Simpson, J.E., Diurnal changes in sea-breeze direction. *J. Applied Meteor.* **1996**, 35, 1166-1169.

Skamarock, W.C.; Klemp, J.; Dudhia, J.; Gill, D.O.; Barker.; D.M., Wang, W.; Powers, J.G. A Description of the Advanced Research WRF Version 2. *NCAR Technical Note*, NCAR/TN-468+STR. Mesoscale and Microscale Meteorology Division, National Center for Atmospheric Research, Boulder, Colorado, USA. **2005**.

Tijm, A.B.C., A.A.M. Holtslag, A.J. Van Delden. Observations and Modeling of the Sea Breeze with the Return Current. Monthly Weather Review **1999**, 127, 625-640.

Zhong, S., and E.S. Takle, An observational study of sea- and land-breeze circulation in an area of complex heating. *J. Atmos. Sci.* **1992**, 31, 1426-1438.

Table 1: Details of WRF ARW model

Model Name	NCAR/NCEP WRF ARW VERSION 3		
Model type	Primitive equation, Non- hydrostatic		
Vertical resolution	41 sigma levels		
Two- way nested three domains			
Horizontal resolution	36 km	12 km	4 km
Domain of integration	93.0 W – 78.05 W 27.16 N – 34. 45 N	91.74 W – 81.92 W 28.5 N – 34. 45 N	90.28 W – 84.77 W 29.38 N – 32.54 N
Number of grids (W-E x S-N)	54 x 40	109 x 76	187 x 118
Radiation	Dudhia scheme for short wave radiation. Rapid Radiative Transfer Model for long wave radiation		
Surface physics	RUC Land- Surface Model		
Sea Surface Temperature	Real Sea Surface Temperatures		
Convection	Kain- Fritsch (KF-Eta).		
PBL	YSU		
Explicit moisture	WSM3 Simple Ice		

Figure 1. Locations of Harrison County School and Wiggins Airport, where special observations were collected during the Joint NOAA/ARL- JSU/TLGVRC Field Experiment- Summer

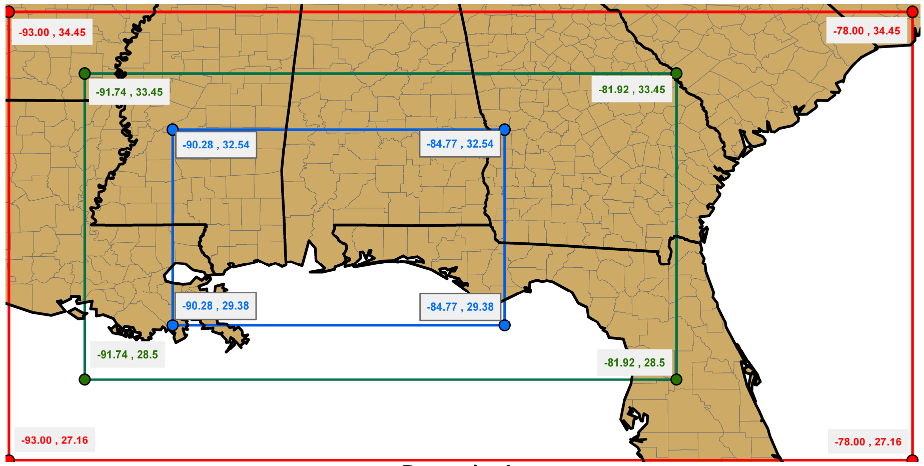

Figure 2. Model domains.

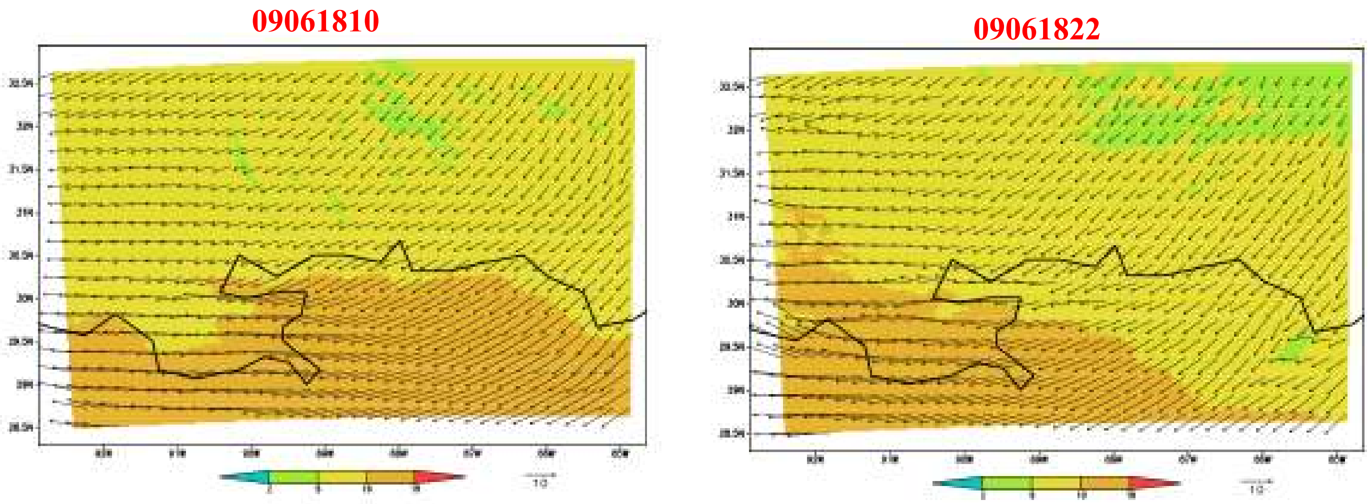

Figure 3. Model simulated wind flow over the Mississippi Gulf Coast region at two different times of 18 June 2009. Wind speed (m/s) is shown as shaded.

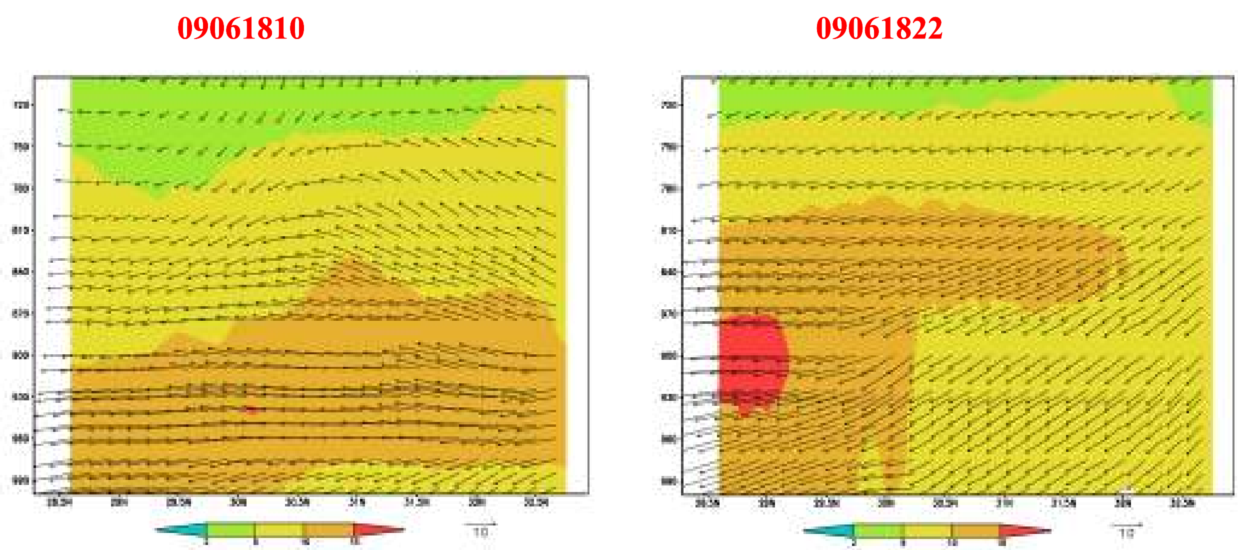

Figure 4. Model simulated latitude- height section of wind flow along 89 W at two different times of 18 June 2009. Wind speed is shown as shaded and wind flow as vectors.

09061810 **09061822**

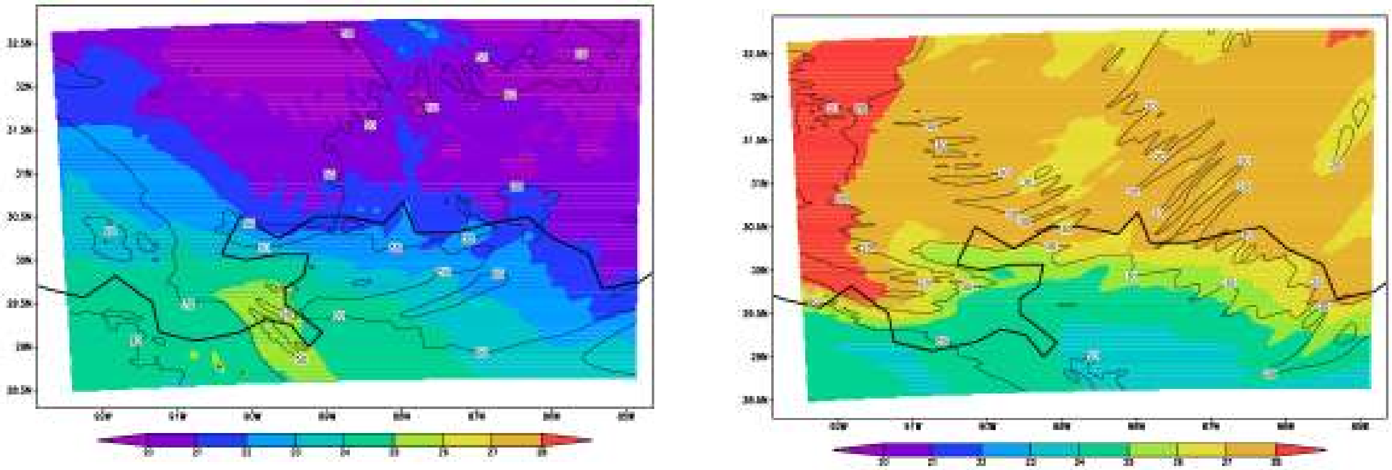

Figure 5. Model simulated temperature (°C) and relative humidity (%) over the Mississippi Gulf Coast region at two different times of 18 June 2009. Temperature is shown as shaded and relative humidity is shown in contours.

09061810 **09061822**

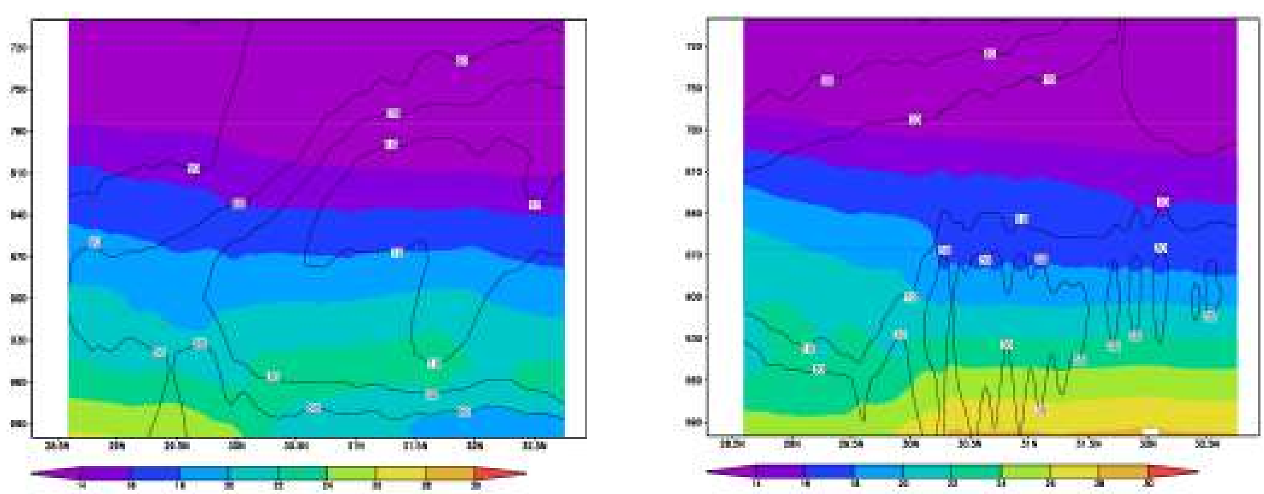

Figure 6. Model simulated latitude- height section of temperature (°C) and relative humidity (%) along 89 W at three different time of 18 June 2009. Temperature is shown as shaded and relative humidity is shown as contours.

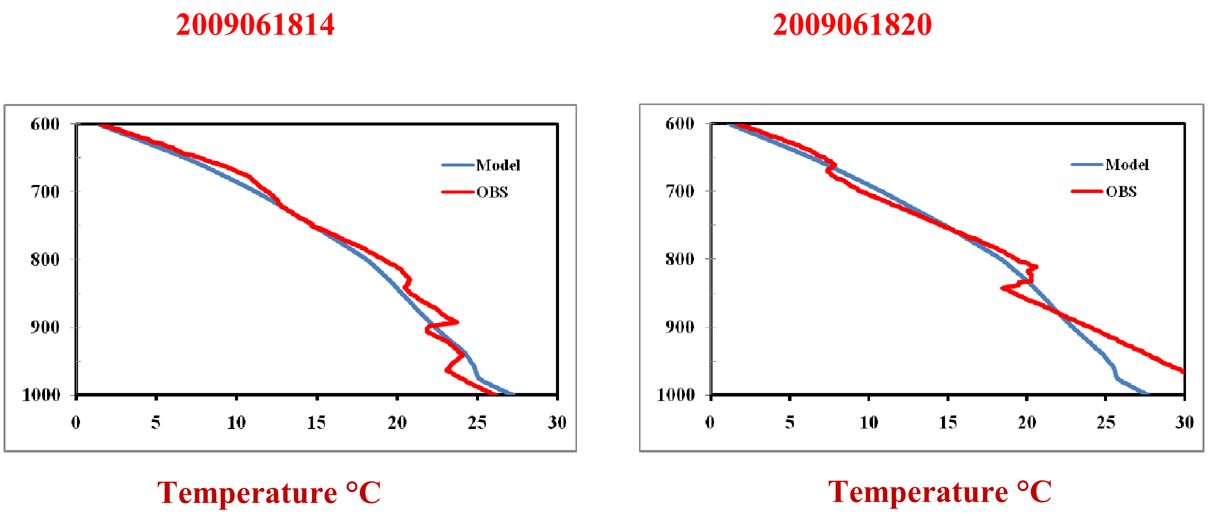

Figure 7. Vertical variation of temperature (°C), model simulated and observed, at Harrison County School at different times on 18 June 2009

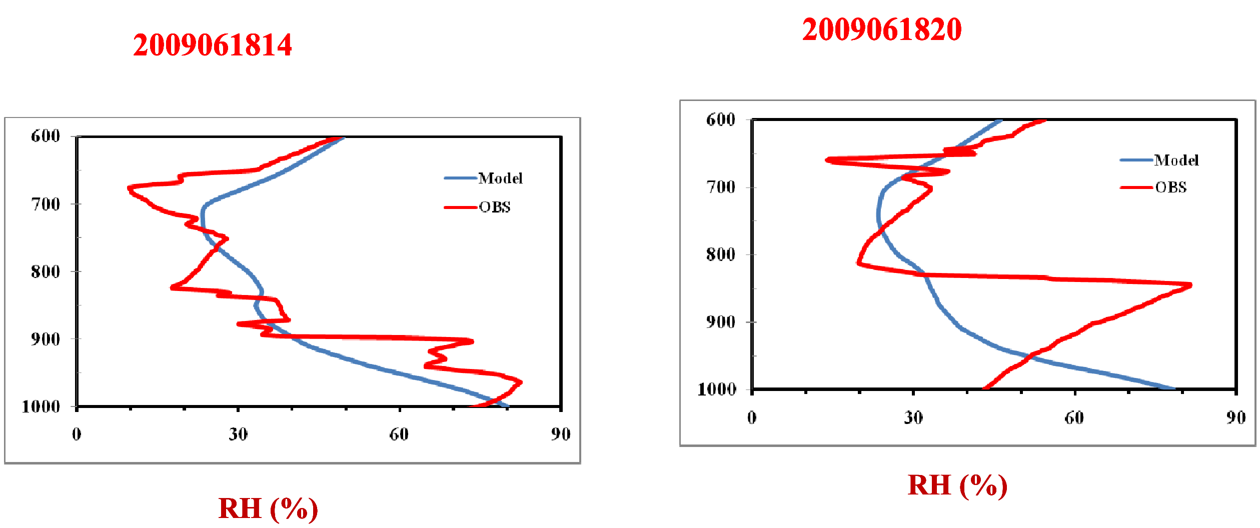

Figure 8. Vertical variation of relative humidity (%), model simulated and observed, at Harrison County School at different times on 18 June 2009

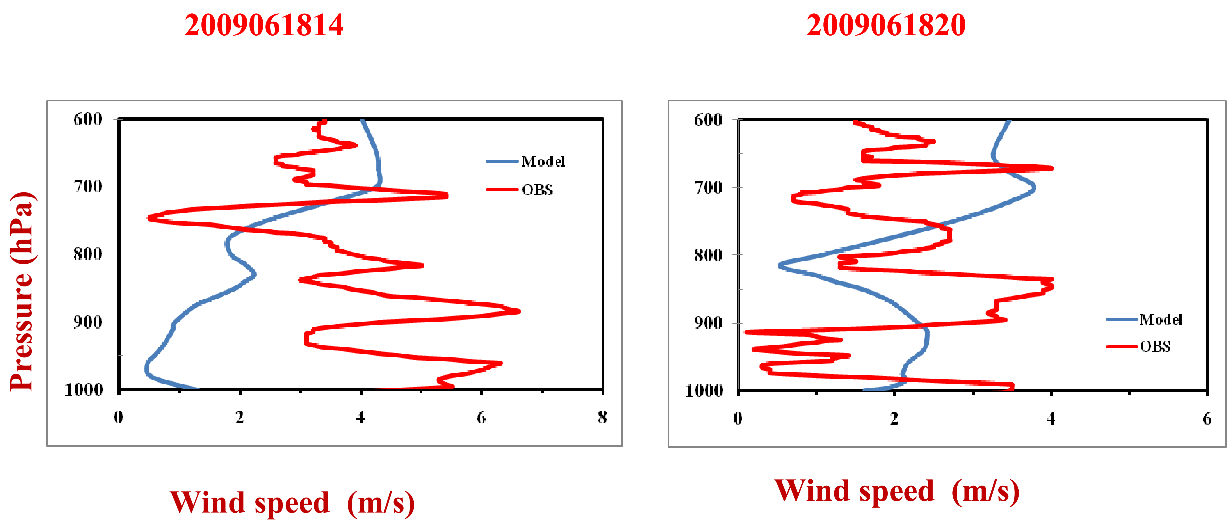

Figure 9. Vertical variation of wind speed (m/s), model simulated and observed, at Harrison County School at different times on 18 June 2009

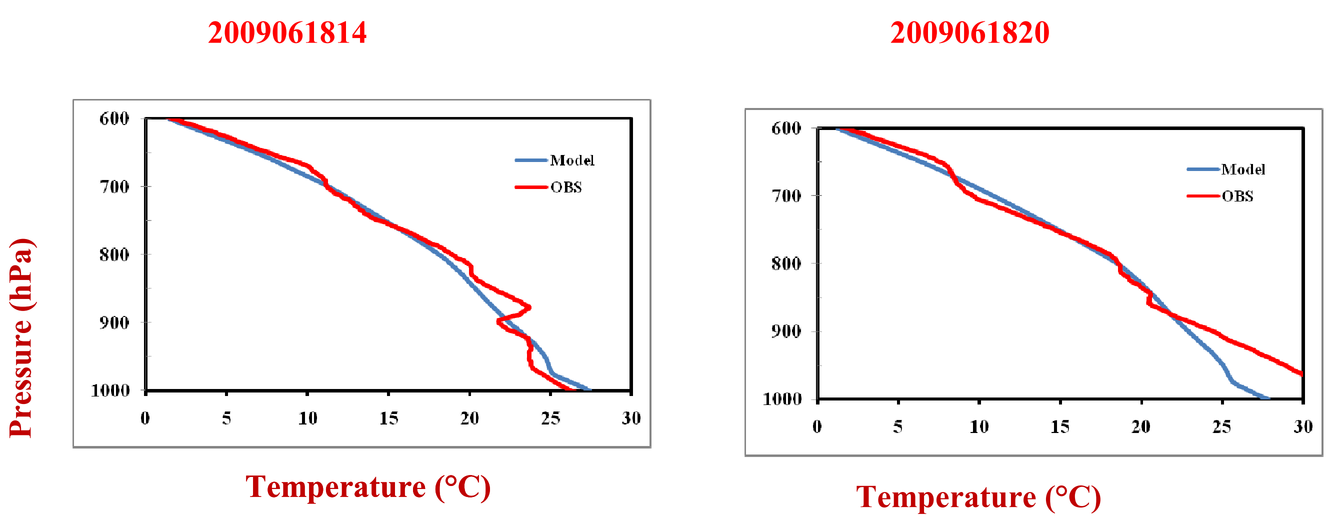

Figure 10. Vertical variation of temperature (°C), model simulated and observed, at Wiggins Airport at different times on 18 June 2009

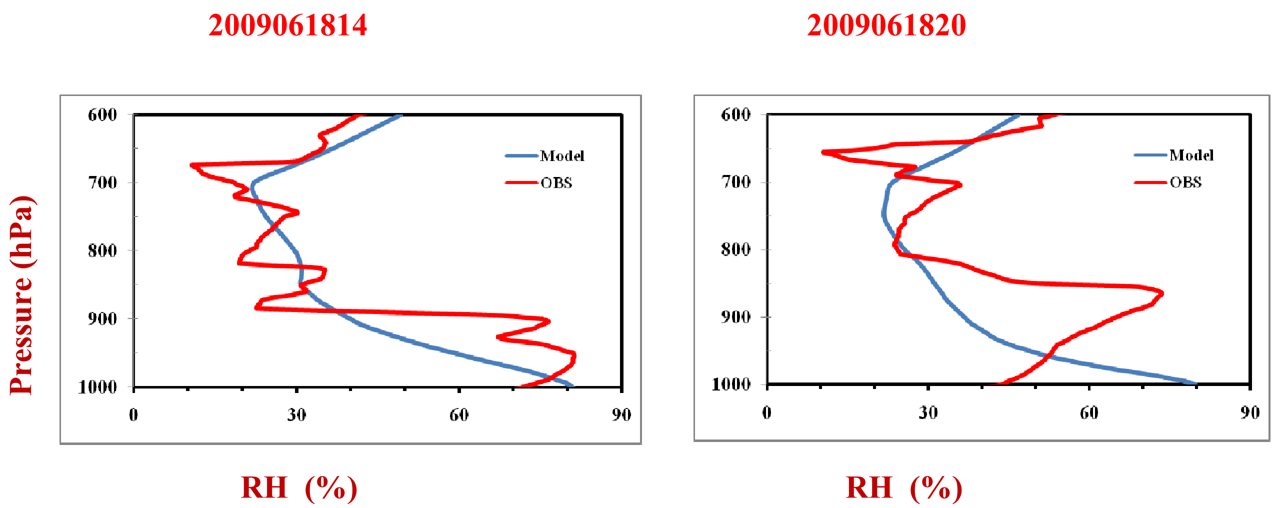

Figure 11. Vertical variation of relative humidity (%), model simulated and observed, at Wiggins Airport at different times on 18 June 2009

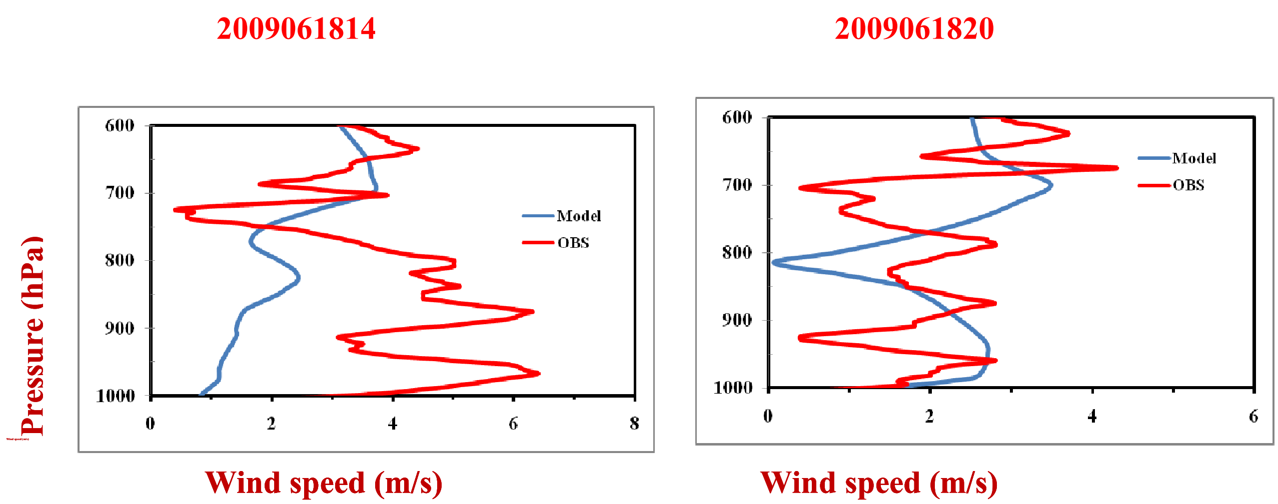

Figure 12. Vertical variation of wind speed (m/s), model simulated and observed, at Wiggins Airport at different times on 18 June 2009